



ELSEVIER

Journal of Alloys and Compounds 333 (2002) 266–273

Journal of
ALLOYS
AND COMPOUNDS

www.elsevier.com/locate/jallcom

Disproportionation of CaNi_3 hydride: formation of new hydride, CaNiH_3

Hiroyuki T. Takeshita^{a,*}, Toshio Oishi^b, Nobuhiro Kuriyama^a^aOsaka National Research Institute, AIST, METI, 1-8-31 Midorigaoka, Ikeda, Osaka 563-8577, Japan^bDepartment of Materials Science and Engineering, Faculty of Engineering, Kansai University, Yamada, Suita, Osaka 564-8680, Japan

Received 16 March 2001; received in revised form 25 June 2001; accepted 25 June 2001

Abstract

The hydrogenation properties of CaNi_3 were investigated at temperatures ranging from 298 to 773 K by differential thermal analysis (DTA). This compound exhibited four exothermic peaks at 373, 498, 543 and 653 K followed by an endothermic peak at 748 K when the compound was heated to 773 K under a hydrogen atmosphere of 3 MPa, and its final products were CaH_2 and Ni. However, the formation of a new ternary hydride was observed in the X-ray diffraction (XRD) profiles below the endothermic reaction temperature at which the final products were formed. The Rietveld refinement of the obtained XRD profiles and a volumetric measurement of the hydrogen content based on the Sieverts' method indicated that this new phase was CaNiH_3 with a cubic CsCl type structure for the metal constituents. The experimental data obtained by XRD and DTA were discussed from the viewpoint of the disproportionation of CaNi_3 in the hydrogen atmosphere. © 2002 Elsevier Science B.V. All rights reserved.

Keywords: Hydrogen storage materials; Powder metallurgy; X-ray diffraction; Phase transitions; Thermal analysis

1. Introduction

The hydrogenation properties of CaNi_3 have been studied by Oesterreicher et al. [1]. The authors reported that CaNi_3 absorbed hydrogen to form its hydride with the composition of $\text{CaNi}_3\text{H}_{4.57}$, with retaining the PuNi_3 type structure [2]. In recent years, the hydrogenation properties obtained by not only the gas–solid reaction but also an electrochemical reaction have been reported for CaNi_3 and its related alloys [3–6]. Some of us have reported that, under moderate conditions such as room temperature and atmospheric pressure, these CaNi_3 -based alloys reversibly absorb and desorb a large amount of hydrogen accompanied by hydrogen pressure plateaus [3,5]. These CaNi_3 -based alloys are attractive as hydrogen storage materials in the coming hydrogen energy era, because of their good hydrogenation properties and relatively low material cost.

In practical use, hydrogen absorption and desorption of these materials are considered to be performed by controlling the temperature rather than hydrogen pressure from the viewpoint of the utilization of waste heat from industry. Some of the alloys lose their reversibility for hydrogen occlusion by decomposing to form stable elemental hydrides at high temperatures [7–9]. Moreover, it is well-

known that some hydrides lose their crystallinity to form amorphous ones by increasing temperature [10–12], which is one of the phenomena observed for hydrogen-induced amorphization (HIA) [13,14]. Thus it is very important and interesting to investigate the hydrogenation properties of materials at high temperatures. However, no information is available for the high temperature hydrogenation properties for CaNi_3 and its related alloys, although it has been reported for its stability for a long time that the hydrogenated sample exposed to air for 1 year is attracted to a magnet, which indicates the precipitation of metallic Ni [1].

The objective of this study was to obtain more extensive data for the hydrogenation characteristics of the CaNi_3 compound at high temperatures up to 773 K (500°C). Their hydrogenation properties and change in crystal structure were analyzed by mainly using differential thermal analysis (DTA) and X-ray diffraction (XRD), respectively.

2. Experimental details

The starting materials included granular Ca (99.5%) and powdered Ni (99.9%). CaNi_2 was prepared in advance as a raw material in order to synthesize the CaNi_3 samples. The Ca granules were cut into fine grains and mixed with Ni

*Corresponding author. Fax: +81-727-51-9629.

E-mail address: hiroyuki-takeshita@aist.go.jp (H.T. Takeshita).

powder so that the total composition was CaNi_2 . The mixtures were then cold-pressed into tablets. The tablets were put into a Mo crucible and the crucible was placed in a stainless steel vessel with a thermocouple inside. Rapid heating of the tablets resulted in the melting of Ca at the Ca– CaNi_2 eutectic temperature (878 K [15]) as found in the Ca–Ni binary phase diagram (Fig. 1), which caused damage to the vessel. In order to avoid this problem, the temperature of the tablets had to be slowly increased at temperatures ranging from 850 to 900 K. As a result of the preliminary evaluation for heating, the programmed temperature control shown in Fig. 2a was applied to the heat treatment of the tablets. The prepared tablets were crushed into powder to check the homogeneity by XRD analysis. The cold-press, heat treatment and pulverization were repeated until samples with the single phase of CaNi_2 were obtained. The CaNi_3 samples were prepared following the same procedure as the CaNi_2 ones, except for the starting materials (powdered CaNi_2 and Ni) and the heat treatment condition (Fig. 2b). All the treatments described above were conducted under an Ar atmosphere.

The crystal and metallographic structures of the samples were examined by XRD analysis using Cu $K\alpha$ radiation and with a scanning electron microscope equipped with a wavelength dispersive X-ray spectroscopy (SEM-WDS), respectively. The apparatus used was a Rigaku RU-200 for the XRD and a Hitachi S-2500CX and Microspec WDX-3PC for the SEM-WDS. Some of the XRD profiles obtained with a step size of 0.02° in 2θ at 298 K (25°C) were analyzed using the Rietveld refinement program 'RIETAN97 β '. The details for this program are described in Refs. [16–18].

The measurements of the hydrogenation properties at high temperature were carefully performed so that the temperature of the alloy sample was not suddenly elevated due to its exothermic reaction. Otherwise the direct

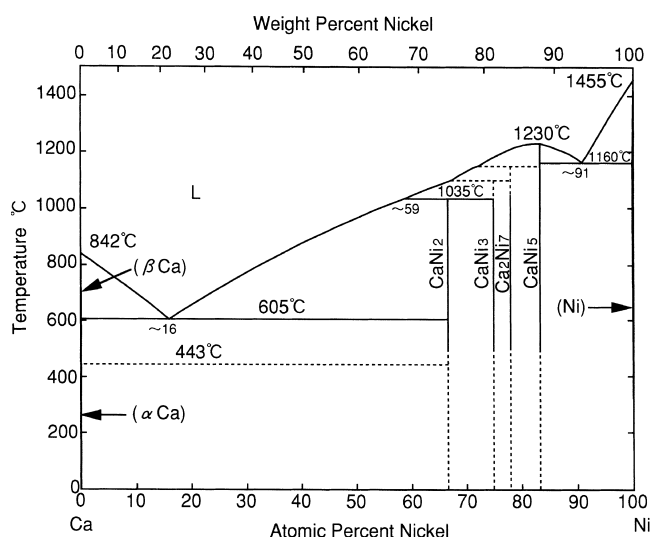


Fig. 1. Binary phase diagram of Ca–Ni system [15].

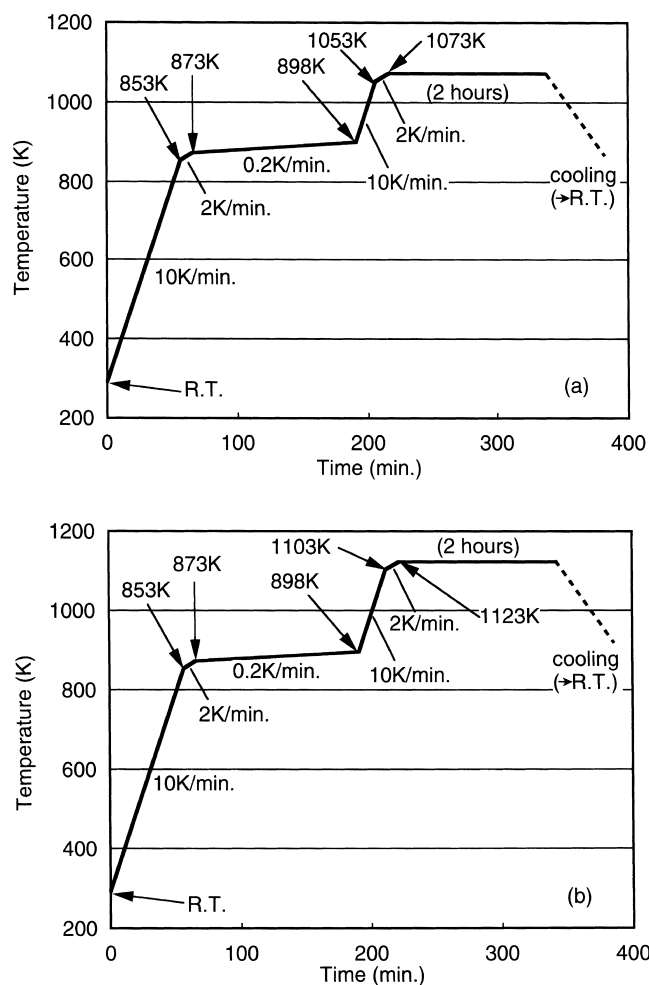


Fig. 2. Schematic diagrams for programmed temperature control on heat treatment of (a) CaNi_2 and (b) CaNi_3 samples.

decomposition of CaNi_3 into CaH_2 and Ni occurred without the formation of an intermediate phase, which was quite different from the results described later.

The reaction of the samples with hydrogen gas were examined by DTA. The DTA apparatus used was a Rigaku DSC8230HP. For the DTA measurements, the samples, each 50 mg, which were exposed to hydrogen gas of 3 MPa, were heated to 773 K (500°C) at the rate of 20 K per min, cooled to 373 K at the same rate and finally cooled to room temperature at a rate depending on the apparatus. A conventional Sieverts'-type apparatus constructed by LESCA was used for the volumetric determination of the hydrogen content in the samples. For these measurements, the samples, each 0.5 g, had been hydrogenated under the conditions of 313 K (40°C) and 2 MPa for 1 day. The samples were carefully heated at 623 K (350°C) for several hours and then cooled to 313 K again. After these treatments, the hydrogen contents were measured at 313 K. The experimental error for the obtained hydrogen content was estimated to be ± 0.02 H/M (H/M; the atomic ratio of hydrogen to metal). It was confirmed by XRD analysis that

the sample prepared for the measurement of the hydrogen content possessed the desired constituent phases.

3. Results

Fig. 3 shows the DTA curve for the hydrogenation of the CaNi_3 sample. The DTA curve showed five peaks with increasing temperature from room temperature to 773 K but no peak during cool down to room temperature except for the false ones due to the variation in the baseline. The first peak (i) around 373 K was the largest and sharp exothermic one. The second one (ii) observed around 498 K was also exothermic and sharp. The exothermic peak (iii), which was small and broad, was observed around 543 K. Peak (iv), which was exothermic, the smallest and very broad, was observed around 653 K. The fifth one (v) around 748 K was endothermic.

In order to estimate the reactions corresponding to these five peaks, the XRD analysis was performed for the samples heated to 473, 523, 573, 673 and 773 K under a hydrogen atmosphere of 3 MPa. The XRD profiles for these samples are shown with the profile for the sample before hydrogenation in Fig. 4. For the sample before the DTA analysis, as shown in Fig. 4a, the diffraction peaks were identified as a PuNi_3 -type structure and no peak from impurity phases was observed, except Si which was mixed with the sample powder as the internal standard material. The lattice constants for the PuNi_3 -type structure were calculated to be $a_0=5.036 \text{ \AA}$ and $c_0=24.32 \text{ \AA}$. These values were in agreement with those reported by Buschow ($a_0=5.030 \text{ \AA}$, $c_0=24.27 \text{ \AA}$) [19]. For the sample heated to 473 K (Fig. 4b), all the diffraction peaks were also

identified as the PuNi_3 -type structure and the standard ones of Si. The lattice constants were calculated to be $a_0=5.455 \text{ \AA}$ and $c_0=26.65 \text{ \AA}$ for the PuNi_3 -type structure. These values were also in agreement with those reported for $\text{CaNi}_3\text{H}_{4.57}$ ($a_0=5.444 \text{ \AA}$, $c_0=26.56 \text{ \AA}$) [1], and therefore, the XRD profile in Fig. 4b indicated the existence of a CaNi_3 hydride. The lattice and volume expansion due to the hydrogenation of CaNi_3 was calculated to be +8.4, +9.8 and +28.6% for a_0 , c_0 and V_0 , respectively. For the sample heated to 523 K, the diffraction peaks from the PuNi_3 -type structure disappeared and a few broad peaks were observed (Fig. 4c). For the sample heated to 573 K, several unidentified peaks appeared in addition to the ones from metallic Ni (Fig. 4d). These peaks became larger and sharper at 673 K (Fig. 4e). The XRD profile for the sample heated to 773 K exhibited the existence of CaH_2 and Ni (Fig. 4f). The sample powders heated to temperatures higher than 523 K were attracted to a magnet, which indicated the existence of metallic Ni in the sample.

The detailed analysis of the unidentified peaks observed in Fig. 4d,e indicated the existence of a new phase with the structure of a simple body-centered cubic (b.c.c.) type. The coexistence of this new phase and Ni was also observed in the hydrogenated CaNi_2 samples [20], which indicated that the composition of the new phase could be expressed as CaNi_{2-x} ($0 < x \leq 2$), where x denotes an unknown number in the present study. One of the local compositions analyzed with the SEM-WDS apparatus was Ca:Ni=1:1.2, although the others were Ca:Ni=1:3. It was expected from this information that this new phase had a simple b.c.c. or CsCl type structure for its constituent metal atoms.

We performed the Rietveld refinement for the XRD profiles of the sample obtained at 673 K. The experimental and calculated profiles are shown with their difference in

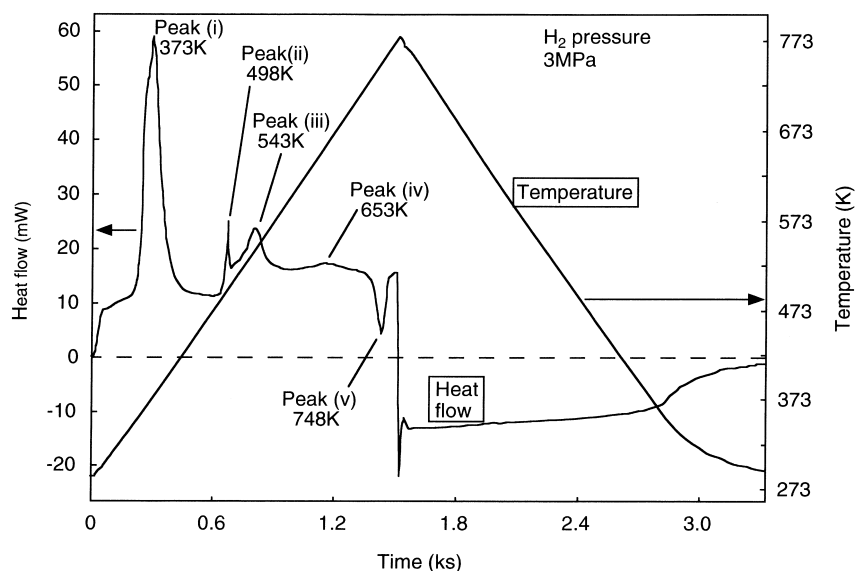


Fig. 3. Results obtained by differential thermal analysis ranging from room temperature to 773 K under hydrogen atmosphere of 3 MPa for CaNi_3 .

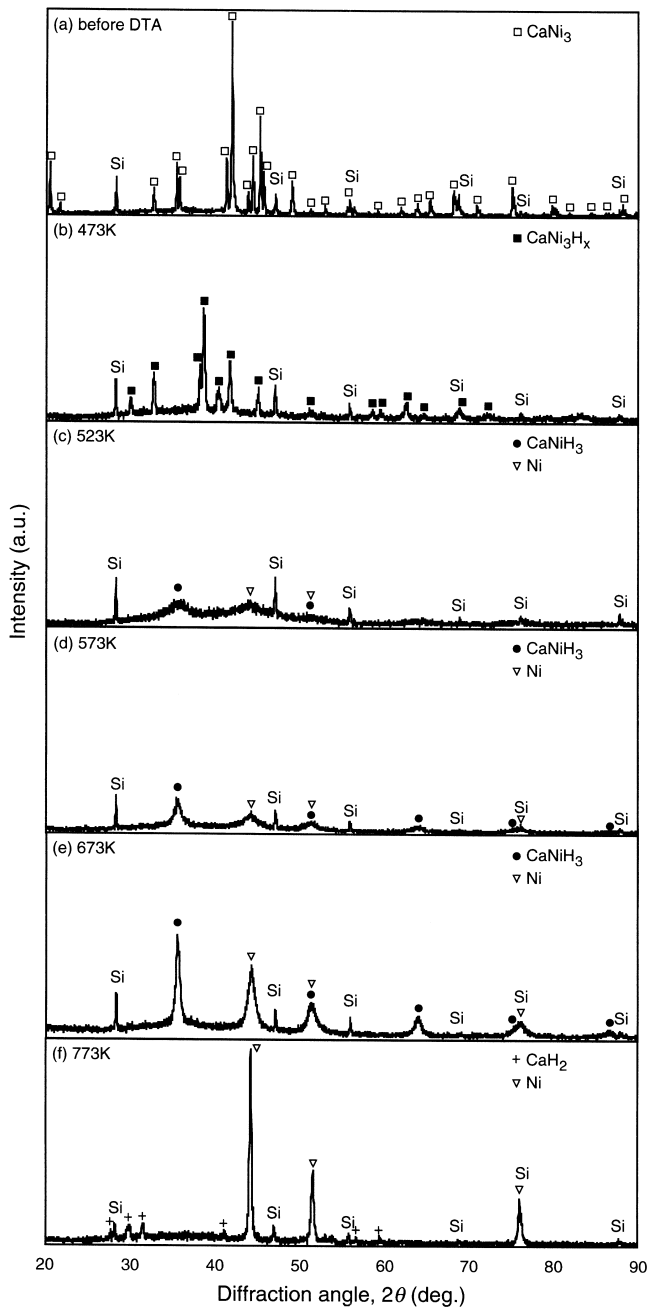


Fig. 4. X-ray diffraction profiles of CaNi_3 samples before differential thermal analysis (a) and after heated to 473 K (b), 523 K (c), 573 K (d), 673 K (e) and 773 K (f) in differential thermal analysis.

Fig. 5. Tables 1 and 2 list the results of the refinement, where a small amount of CaH_2 was included in the sample supplied to the Rietveld refinement. The results of the refinement indicated that the CsCl type structure was much more possible than the b.c.c. one, as could be easily found from the (100) peak corresponding to the ordered lattice peak of the CsCl type one, shown by an arrow in Fig. 5. The $1a$ and $1b$ positions were fully occupied by Ca and Ni atoms, respectively, so the composition of the new phase for metal elements was $\text{Ca}:\text{Ni}=1:1$.

The hydrogen contents of the samples heated at 473 and 623 K were measured at 313 K with a Sieverts'-type apparatus. The hydrogen contents at 313 K for these samples are listed in Table 3. The hydrogen content at 313 K and 2 MPa was 0.76 ± 0.02 H/M for the sample heated at 623 K, which corresponded to $\text{CaNi}_3\text{H}_{3.0}$ in overall composition. It was confirmed by XRD analysis that the constituent phases of this sample were metallic nickel and the CsCl-type phase which can be expressed as CaNiH_x . Based on the assumption that metallic Ni did not react with hydrogen under the present conditions, the value of x was found to be 3.0 from the following relation



Therefore, it was found that the new phase was CaNiH_3 with a cubic CsCl type structure for the constituent metal atoms.

The new hydride CaNiH_3 has a large hydrogen capacity for not only the atomic ratio (1.5 H/M) but also for the weight ratio (3 wt%). Since the intermetallic compound phase with the composition of $\text{Ca}:\text{Ni}=1:1$ is not formed as

Table 1

Lattice constant of each constituent phase in the sample heated to 673 K under hydrogen atmosphere of 3 MPa, obtained by Rietveld refinement of its X-ray diffraction profile at 298 K

Phase	Space group	a_0 (Å)	b_0 (Å)	c_0 (Å)	R_B (%)	R_F (%)
CaNiH_3	$Pm\bar{3}m$	3.5518(2)			1.78	1.00
Ni	$Fm\bar{3}m$	3.5285(3)			1.07	0.52
CaH_2	$Pnma$	5.936(9)	3.594(4)	6.770(9)	1.50	0.83

Estimated standard deviations in parentheses; $R_{wp} = 8.10\%$, $R_p = 5.97\%$, $R_e = 6.37\%$.

Table 2

Crystallographic parameters for constituent metal atoms of CaNiH_3 obtained by Rietveld refinement of X-ray diffraction profile

Atom	Site	x	y	z	Occupancy
Ca	$1a$	0	0	0	1.00(1)
Ni	$1b$	1/2	1/2	1/2	0.998(8)

Estimated standard deviations in parentheses; B_{iso} values are fixed for both Ca (0.17 \AA^2) and Ni (1.13 \AA^2).

Table 3

Hydrogen contents at 313 K and 2 MPa hydrogen pressure for samples which are heated to 473 and 623 K and their constituent phases after heat treatment

Constituent phases before hydrogenation	Treatment temperature (K)	Hydrogen content (H/M)	Constituent phases after hydrogenation
CaNi_3	473	1.10(2)	$\text{CaNi}_3\text{H}_{4.4}$
CaNi_3	623	0.76(2)	CaNiH_3 , Ni

Experimental errors in parentheses.

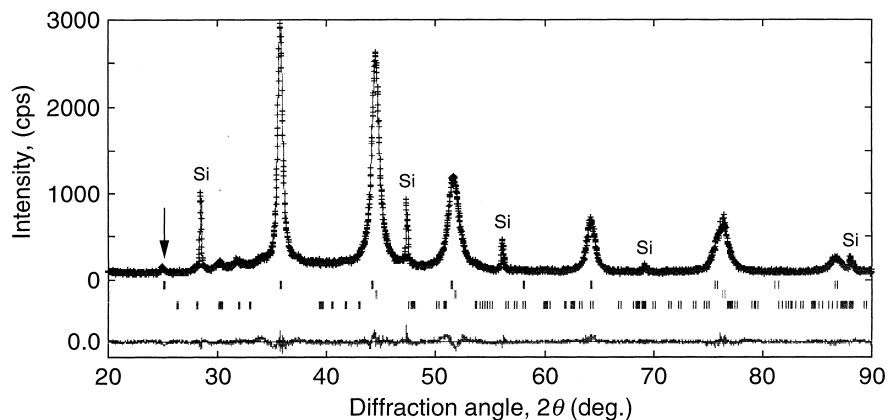


Fig. 5. Rietveld profile refinement of X-ray diffraction profile measured at 298 K for sample heated to 673 K at 3 MPa; profile observed (top), calculated CaNiH_3 , Ni and CaH_2 (middle) and difference (bottom). Arrow indicates (100) ordered lattice peak of CaNiH_3 with CsCl type structure for constituent metal atoms.

an equilibrium one as seen in Fig. 1 [15], it can be said that this new hydride is the phase stabilized by hydrogen atoms, that is, the hydrogen-stabilized phase.

4. Discussion

4.1. Comparison of CaNiH_3 with hydrides of MgNi and YbNi

Orimo et al. have reported that an amorphous MgNi and its hydride have local structures related to the CsCl type structure [21,22]. Taking into account the fact that Mg is an alkaline-earth element as well as Ca, it can be expected that CaNi and MgNi hydrides have some similarities with respect to their crystallographic structures. Therefore, the present result for the CaNi hydride obtained by the Rietveld refinement supports their results for the amorphous MgNi hydride. However, there are differences between the hydrogenation properties of the CaNi and MgNi hydrides. The hydrogen content of the CaNi hydride is 1.5 H/M which is much higher than that of MgNi (about 1 H/M [21,23]). In addition, the CaNi does not show any reversibility for the reaction with hydrogen gas, although the MgNi exhibits a reversible hydrogenation and dehydrogenation.

The hydrogen content and lattice constant of CaNiH_3 were compared with those for the hydride of YbNi [24].

Table 4
Comparison of structural data for CaNiH_3 with that for $\text{YbNiH}_{2.7}$ [24]

Composition	Crystal structure ^a	Goldschmidt radius (Å)	Lattice constant (Å)
$\text{CaNiH}_{3.0}$ ^b	CsCl type ^b	1.97 (Ca)	3.5518(2) ^b
$\text{YbNiH}_{2.7}$	CsCl type	1.94 (Yb)	3.55

^a For constituent metal atoms.

^b Present work.

The compositions, Goldschmidt radii, crystal structures for metal constituents and lattice constants for both hydrides are listed in Table 4. The Goldschmidt radius of Ca is approximately equal to that of Yb and both hydrides have the same structures for the constituent metal atoms. The obtained hydrogen content and lattice constant for the hydride of CaNi are comparable to those for the YbNi hydride, respectively.

Oesterreicher et al. described that the hydrogen uptake of the compounds in the Ca–Ni system was given by the weighted hydrogen uptake of the elemental Ca and Ni hydrides [1], that is, the hydrogen uptake x of $\text{Ca}_a\text{Ni}_b\text{H}_x$ can be given to be $2a + 0.7b$ from the following equation,

$$\text{Ca}_a\text{Ni}_b\text{H}_x = a \cdot \text{CaH}_2 + b \cdot \text{NiH}_{0.7},$$

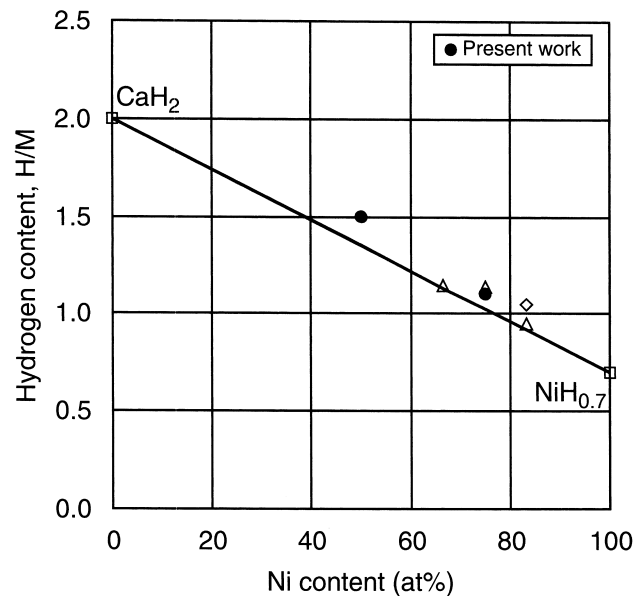


Fig. 6. Relation between hydrogen uptake and Ni content of Ca–Ni-based compounds. Data are taken from Refs. [1,26–28] and present results.

where a and b are constants. Fig. 6 shows the change in hydrogen uptake of the Ca–Ni compounds with their compositions for the constituent metal elements. As seen in Fig. 6, CaNiH_3 obeys the rule that the maximum hydrogen content of each compound lies close to the straight line connecting the hydrogen contents of the two elemental hydrides, CaH_2 and $\text{NiH}_{0.7}$. Also, this rule has been reported for some rare earth(R)–transition metal(T) systems [25].

Thus the hydrogenation and crystallographic properties of CaNiH_3 are similar to some extent to those of both amorphous MgNi and crystalline RNi . This implies that the substitution of a variety of elements for Ca can be applied to the modification of the CaNiH_3 . In fact, the effect of the substitution of rare earth elements and Mg for Ca on the hydrogenation properties has been investigated for CaNi_3 [5]. The effect of the elemental substitution on the hydrogenation properties of CaNiH_3 will be described in other papers.

4.2. Procedure for decomposition of CaNi_3 under a hydrogen atmosphere

The XRD profiles in Fig. 4a,b show the existence of the CaNi_3 compound and its hydride, respectively, which indicate that the hydrogenation of the CaNi_3 compound is responsible for the largest exothermic peak (i) observed in Fig. 3. From the comparison of the XRD profile in Fig. 4d with the one in Fig. 4e, peak (iv) is attributed to the growth of CaNiH_3 and Ni crystallites. The XRD profiles in Fig. 4e,f show the coexistence of the CaNiH_3 and Ni and the coexistence of CaH_2 and Ni, respectively, which indicates that the decomposition of CaNiH_3 into CaH_2 and Ni is responsible for peak (v) observed in Fig. 3. In this decomposition, the total hydrogen amount in the sample decreases from CaNi_3H_3 ($\text{CaNiH}_3 + 2\text{Ni}$) to CaNi_3H_2 ($\text{CaH}_2 + 3\text{Ni}$). Therefore, the endothermic heat of peak (v) is attributed to the hydrogen desorption accompanying the decomposition.

From the comparison of the XRD profile in Fig. 4c with the one in Fig. 4d, it can be judged that the broad peaks observed in Fig. 4c correspond to the strong ones such as those from the (110) and (211) planes for CaNiH_3 and the (111) plane for Ni in Fig. 4d. The existence of Ni in the sample heated to 523 K is also confirmed by the fact that the sample powder is attracted to a magnet. Therefore, the precipitation of these phases is considered to start below 523 K. We have two possible explanations for the reactions which are responsible for peaks (ii) and (iii). One is that peaks (ii) and (iii) are attributed to the disproportionation of the CaNi_3 hydride into CaNiH_3 and Ni and the growth of these two phases, respectively. In this case, the crystallites of CaNiH_3 and Ni grow during two different steps because both peaks (iii) and (iv) are responsible for the growth of these crystallites. Another possible explanation is that the reactions corresponding to these peaks are the

amorphization of the crystalline CaNi_3 hydride, so-called hydrogen-induced amorphization (HIA), and the formation of CaNiH_3 and Ni from the amorphous hydride, respectively. In this case, it can be explained that, since the exothermic heat due to reaction (ii) triggers reaction (iii), the crystalline phases are observed in Fig. 4c.

Since the PuNi_3 type structure of CaNi_3 partially contains the Laves one [29,30], we assume that the information about interatomic diffusion in the Laves compounds can be applied to the diffusion in CaNi_3 . It has been reported for MgCu_2 type RCO_2 compounds that the ratios of their crystalline hydride formation temperatures (T_h), amorphization ones (T_a) and crystallization (formation of elemental hydrides) ones (T_x) to the corresponding melting (decomposition) points (T_m), that is T_h/T_m , T_a/T_m and T_x/T_m , are respectively, 0.28, 0.40 and 0.5 [12]. The growth of crystallites from the mixture of very small ones of two phases requires an interatomic diffusion over a long distance and the growth of crystallites occurs at temperatures higher than T_x [12]. Therefore, the temperature ratio for the growth of crystallite is greater than 0.5. The ratio of the temperature of peak (iv) (T_{iv}), corresponding to the growth of CaNiH_3 and Ni, to the peritectic melting point of CaNi_3 (T'_m) (=1287 K [31]), T_{iv}/T'_m , is 0.51 which is in agreement with the reported information. On the other hand, the ratios T_{iii}/T'_m and T_{ii}/T'_m are only 0.42 and 0.39, which are much smaller even compared with T_x/T_m . This implies that the reaction based on the long-range interatomic diffusion such as the growth of crystallites does not easily occur at T_{iii} . Moreover, the value of T_{ii}/T'_m (0.39) is approximately equal to T_a/T_m at which the interatomic diffusion could occur over a limited short range [12]. This can indicate the disproportionation of CaNi_3 hydride into CaNiH_3 and Ni that requires higher temperatures than T_{ii} . Thus the former proposal seems to be inadequate as a possible explanation for the reactions causing peaks (ii) and (iii). On the other hand, the amorphization at T_{ii} is possible because the value of the T_{ii}/T'_m is about 0.4. The T_{iii}/T'_m value (=0.42) is intermediate between T_a/T_m and T_x/T_m . At this temperature, interatomic diffusion is expected to be still limited, but can occur over a longer range than that in HIA. The decomposition into CaNiH_3 and Ni requires a longer-range interatomic diffusion than HIA and is expected to occur by interatomic diffusion in the limited range compared with that into CaH_2 and Ni in which Ca and Ni are completely separated from each other. Thus the disproportionation of the amorphous CaNi_3 hydride into CaNiH_3 and Ni can be considered to occur at T_{iii} .

As is well-known, the materials with atomic size ratios larger than 1.1 form their corresponding amorphous phases by rapid quenching [32]. Aoki and Masumoto have shown that all the MgCu_2 type Laves RT_2 compounds with Goldschmidt radius ratio, R_R/R_T , values larger than 1.37 undertake HIA [13]. Thus a large atomic size ratio for the constituent elements of the material is required for the formation of its corresponding amorphous phase. Raj and

Shashikala have described that the intermetallic compounds showing HIA are either metastable or peritectic in their corresponding phase diagram [14]. For CaNi_3 showing peritectic melting (see Fig. 1), the Goldschmidt radii of Ca and Ni are 1.97 and 1.25, respectively, and the value of $R_{\text{Ca}}/R_{\text{Ni}}=1.58$, which is much larger than 1.37. This extremely large atomic size ratio for the Ca–Ni alloys may cause the HIA behavior of CaNi_3 .

Based on the discussion described above, we propose that the HIA and crystallization to form CaNiH_3 and Ni as the most possible reactions which are responsible for exothermic peaks (ii) and (iii), respectively. The hydrogenation of CaNi_3 at elevated temperatures can be summarized below, peak (i) at 373 K; hydrogenation to form crystalline CaNi_3H_x peak (ii) at 498 K; transformation of crystalline to amorphous CaNi_3H_x peak (iii) at 543 K; crystallization of CaNi_3H_x to form CaNiH_3 and Ni peak (iv) at 653 K; growth of crystallites of CaNiH_3 and Ni peak (v) at 748 K; disproportionation of CaNiH_3 into CaH_2 and Ni.

As far as we know, there is no report for the HIA behavior of Ca-based intermetallic compounds and a few reports for the materials with the PuNi_3 type structure except LaNi_3 [25]. Therefore, further examinations are required to confirm the hydrogenation and decomposition procedure proposed in the present study.

5. Conclusion

Using differential thermal analysis, X-ray diffraction and a volumetric measurement of the Sieverts method, the decomposition procedure of CaNi_3 under a hydrogen atmosphere has been investigated in the range between room temperature and 773 K. The obtained results are summarized below.

(1) We suggest that CaNi_3 reacts with hydrogen and decomposes in the following five steps;

- (i) Hydrogenation of CaNi_3 to form its crystalline hydride.
- (ii) Amorphization of crystalline CaNi_3 hydride (hydrogen-induced amorphization)
- (iii) Decomposition of amorphous CaNi_3 hydride to form CaNi hydride and Ni
- (iv) Growth of crystallites of CaNi hydride and Ni
- (v) Disproportionation of CaNi hydride into CaH_2 and Ni

(2) The crystal structure and hydrogen absorbing capacity are determined for a hydrogen-stabilized new ternary hydride using the Rietveld refinement program and a Sieverts'-type apparatus. The crystal structure and hydrogen capacity are a cubic CsCl type structure with the lattice constant of 3.5518(2) Å and 1.5 H/M (3 wt%), respectively. The hydrogen content of CaNiH_3 is approxi-

mately equal to the weighted hydrogen uptake of the elemental hydrides ($\text{CaH}_2 + \text{NiH}_{0.7} = \text{CaNiH}_{2.7}$), which is consistent with the suggestion of Oesterreicher et al. [1].

Acknowledgements

Authors would like to express their sincere thanks to Mr. T. Nakahata for his advice and help in the preparation of the CaNi_3 samples. We wish to also thank Professor K. Aoki of Kitami Institute of Technology for his useful advice.

References

- [1] H. Oesterreicher, K. Ensslen, A. Kerlin, E. Bucher, Mater. Res. Bull. 15 (1980) 275.
- [2] K.H.J. Buschow, J. Less-Common Met. 38 (1974) 95.
- [3] K. Kadir, N. Kuriyama, T. Sakai, I. Uehara, L. Eriksson, J. Alloys Comp. 284 (1999) 145.
- [4] K. Kadir, T. Sakai, I. Uehara, J. Alloys Comp. 287 (1999) 264.
- [5] J. Chen, H.T. Takeshita, H. Tanaka, N. Kuriyama, T. Sakai, I. Uehara, M. Haruta, J. Alloys Comp. 302 (2000) 304.
- [6] J. Chen, N. Kuriyama, H.T. Takeshita, H. Tanaka, T. Sakai, M. Haruta, Electrochem. Solid-State Lett. 3 (2000) 249.
- [7] K. Yamanaka, H. Saito, M. Someno, J. Chem. Soc. Japan (in Japanese) 8 (1975) 1267.
- [8] V.I. Mikheeva, M.E. Kost, A.L. Shilov, Russ. J. Inorg. Chem. 23 (1978) 657.
- [9] V.N. Verbetsky, S.N. Klyamkin, A.Yu. Kovriga, A.P. Bespalov, Int. J. Hydrogen Energy 21 (1996) 997.
- [10] X.L. Yeh, K. Samwer, W.L. Johnson, Appl. Phys. Lett. 42 (1983) 242.
- [11] K. Aoki, X.-G. Li, T. Hirata, E. Matsubara, Y. Waseda, T. Masumoto, Acta Metall. Mater. 41 (1993) 1523.
- [12] K. Mori, K. Aoki, T. Masumoto, Mater. Sci. Eng. A179–A180 (1994) 181.
- [13] K. Aoki, T. Masumoto, J. Alloys Comp. 194 (1993) 251.
- [14] P. Raj, K. Shashikala, Met. Mater. Processes 11 (1999) 329.
- [15] T.B. Massalski, J.L. Murray, L.H. Bennett, H. Baker (Eds.), Binary Alloy Phase Diagrams, American Society for Metals, Metals Park, OH, 1986.
- [16] F. Izumi, in: R.A. Young (Ed.), The Rietveld Method, International Union of Crystallography, Oxford University Press, Oxford, 1993, Ch. 13.
- [17] F. Izumi, Rigaku-Denki J. (in Japanese) 34 (1996) 18.
- [18] F. Izumi, <http://www.nirim.go.jp/~izumi/>
- [19] K.H.J. Buschow, J. Less-Common Met. 38 (1974) 95.
- [20] H.T. Takeshita et al., to be published.
- [21] S. Orimo, K. Ikeda, H. Fujii, S. Saruki, T. Fukunaga, A. Züttel, L. Schlapbach, Acta Mater. 46 (1998) 4519.
- [22] S. Orimo, K. Ikeda, H. Fujii, S. Saruki, T. Fukunaga, Mater. Trans. JIM 63 (1999) 959.
- [23] S. Orimo, H. Fujii, K. Ikeda, Y. Fujikawa, Y. Kitano, J. Alloys Comp. 253–254 (1997) 94.
- [24] K. Ensslen, E. Bucher, H. Oesterreicher, J. Less-Common Met. 92 (1983) 343.
- [25] H. Oesterreicher, J. Clinton, H. Bittner, Mater. Res. Bull. 11 (1976) 1241.
- [26] G.D. Sandroock, J.J. Murray, M.L. Post, J.B. Taylor, Mater. Res. Bull. 17 (1982) 887.
- [27] C.B. Magee, in: W.M. Mueller, J.P. Blackledge, G.G. Libowitz

- (Eds.), *Metal Hydrides*, Academic Press, New York, 1968, pp. 165–240.
- [28] B. Siegel, G.G. Libowitz, in: W.M. Mueller, J.P. Blackledge, G.G. Libowitz (Eds.), *Metal Hydrides*, Academic Press, New York, 1968, pp. 545–674.
- [29] V.A. Yartys', V.V. Burnasheva, K.N. Semenko, N.V. Fadeeva, S.P. Solov'ev, *Int. J. Hydrogen Energy* 7 (1982) 957.
- [30] B.D. Dunlap, P.J. Viccaro, G.K. Shenoy, *J. Less-Common Met.* 74 (1980) 75.
- [31] M. Notin, D. Belbacha, M. Rahmane, J. Hertz, G. Saindrenan, J.L. Jorda, *J. Less-Common Met.* 162 (1990) 221.
- [32] B.C. Giessen, in: T. Masumoto, K. Suzuki (Eds.), *Proc. 4th Int. Conf. on Rapidly Quenched Metals*, Vol. 1, Japan Institute of Metals, Sendai, 1982.